10-1996

Modeling Nutrient and Plankton Processes in the California Coastal Transition Zone: 3. Lagrangian Drifters

J. R. Moisan
Old Dominion University

Eileen E. Hofmann
Old Dominion University, ehofmann@odu.edu

Original Publication Citation

Moisan, J.R., & Hofmann, E.E. (1996). Modeling nutrient and plankton processes in the california coastal transition zone .3. Lagrangian drifters. *Journal of Geophysical Research 101*(C10), 22693-22704. doi: 10.1029/96jc01720

JOURNAL OF GEOPHYSICAL RESEARCH, VOL. 101, NO. C10, PAGES 22,693–22,704, OCTOBER 15, 1996

Modeling nutrient and plankton processes in the California coastal transition zone 3. Lagrangian drifters

J. R. Moisan[1] and E. E. Hofmann
Center for Coastal Physical Oceanography, Department of Oceanography,
Old Dominion University, Norfolk, Virginia

Abstract. Two types of numerical Lagrangian drifter experiments were conducted, using a set of increasingly complex and sophisticated models, to investigate the processes associated with the plankton distributions in the California coastal transition zone (CTZ). The first experiment used a one-dimensional (1-D; vertical) time-dependent physical-bio-optical model, which contained a nine-component food web. Vertical velocities, along the track of simulated Lagrangian drifters, derived from a three-dimensional (3-D), primitive equation circulation model developed to simulate the flow observed within the CTZ, were used to parameterize the upwelling and downwelling processes. The second experiment used 880 simulated Lagrangian drifters from a 3-D primitive equation circulation model which was coupled to the same food web and bio-optical model used in the first experiment. Parameterization of the biological processes in both experiments were based upon data obtained during the CTZ field experiments. Comparison of simulations with data provided insight into the role of the biological and physical processes in determining the development of the subsurface chlorophyll maximum and other related features. In both studies, the vertical velocities experienced by a simulated Lagrangian drifter as it was advected offshore while entrained within a filament played a major role in determining the depth to which the euphotic zone and the chlorophyll maximum developed. Also, as the drifters moved offshore, the food web changed from a coastal, neritic food web to an offshore, oligotrophic food web due to the decrease in nutrient availability. The temporal development of the food web constituents following the simulated drifters was dependent upon the environment to which the drifter was exposed. For example, the amount of time upwelled or downwelled and the initial location in the CTZ region greatly affected the development of the food web.

1. Introduction

The coastal transition zone (CTZ) is a region off the coast of California which is characterized by the presence of cross-shelf jets or filaments [*Brink and Cowles,* 1991]. As these filaments develop, they entrain recently upwelled water near the coast and transport it offshore. As a result, the circulation processes within the CTZ determine and control the interactions between the coastal and offshore ecosystems. The food webs in the water entrained within the filament are observed to undergo a transition from a coastal, neritic environment to an offshore, oligotrophic environment as the filaments advect the water parcel offshore [*Abbott et al.,* 1990].

In the past few years there has been an increase in the use of Lagrangian drifters as tools to obtain data on ocean currents [*Flament,* 1986; *Niiler et al.,* 1989; *Paduan and Niiler,* 1990; *Davis,* 1985a, b], temperature [*Paduan and Niiler,* 1993], salinity, sea surface pressure [*Data Buoy Cooperation Panel,* 1993], and more recently fluorescence, submarine irradiance, and beam transmission [*Abbott et al.,* 1990]. Biologists have used Lagrangian drifters as tools to follow water parcels, thereby allowing them to sample the water column in a semicontinuous and semi-Lagrangian fashion and estimate changes in population growth rates [*Abbott et al.,* 1990]. While sampling in this manner ignores the contributions from vertical and horizontal shear and advection within the water column, it does provide high-resolution measurements along a specific trajectory.

There have been many studies that have used Lagrangian drifters to characterize the currents within the CTZ region. *Davis* [1985a, b] used 164 current-following

[1]Now at Physical Oceanography Research Division, Scripps Institution of Oceanography, La Jolla, California.

Paper number 96JC01720.
0148-0227/96/96JC-01720$09.00

drifters to describe the two-dimensional structure of the mean surface flow in a region centered offshore and south of Point Arena, the region where filaments are observed to occur. His results show that the frontal regions associated with the offshore flowing filaments are regions of convergence, since drifters tended to collect along the fronts. In a similar study off of Point Arena, *Swenson et al.* [1992] deployed 56 TRISTAR-II mixed-layer drifters within the offshore flowing regions of a filament which had formed offshore. Their results also showed that the offshore flowing region of the filament was convergent. In this region, the drifters encountered both large horizontal velocities (greater than 0.1 m s^{-1}) and downwelling velocities (approximately 20 m d^{-1}). The observation of this subduction process was further verified by *Brink et al.* [1991], who deployed 77 near-surface satellite tracked drifters within the cold filaments near Point Arena. Downwelling velocities observed in this study averaged in the order of 10 m d^{-1} at a distance of about 200 km from shore. Finally, *Paduan and Niiler* [1990] released 12 TRISTAR-II drifters in an offshore-flowing portion of a jet off Point Reyes. Their results demonstrated that strong horizontal offshore-flowing currents (greater than 0.5 m s^{-1}) were observed along the axis of the filaments and that these regions were also areas of strong convergence, which is consistent with other observations in this region.

Lagrangian drifters were also used in the CTZ study to guide sampling of the chemical, biological, and optical properties of the water column. *Abbott et al.* [1990] released a TRISTAR-II drifter, equipped with an optical package, a thermistor chain and a water sampler, into the central region of the nearshore end of a filament that was observed to have developed off the California coast. The drifter was tracked for 8 days as it moved offshore while being advected within the offshore flowing portion of the observed filament. The results from this study characterize the time development of a typical upwelling ecosystem. At the beginning of the study, the water mass that the drifter sampled contained high concentrations of nutrients and low concentrations of phytoplankton biomass. Over the course of the next 2 days, the nutrient concentrations decreased rapidly as a result of a rapid growth in the phytoplankton population. In fact, both phytoplankton cell volume and chlorophyll fluorescence were observed to double during the first 2 days. For the remaining 6 days that the drifter was tracked, the nutrient and phytoplankton populations declined slowly. As the drifter moved offshore, the phytoplankton assemblage became progressively dominated by the slow growing large centric diatoms (i.e., *Actinocyclus* and *Thalassiosira* spp.) due to the disappearance of the faster growing chain-forming diatoms (i.e. *Chaetoceros*).

This paper is the third of a series of three studies that were conducted using a set of increasingly complex and sophisticated physical-bio-optical models. This third paper presents the results from two types of simulated Lagranian drifter experiments. The first experiment uses a one-dimensional (1-D, vertical) time-dependent physical-bio-optical model [*Moisan and Hofmann,* this issue]. By using a 1-D model, we were able to isolate the effect of vertical motion from the 3-D circulation field.

The vertical velocities which were used to advect the model constituents were obtained from simulated Lagrangian drifters whose vertical velocities resemble those observed within the CTZ filaments [*Hofmann et al.,* 1991]. The second experiment used simulated Lagrangian drifters from a 3-D, time-dependent, physical-bio-optical model [*Moisan et al.,* this issue]. In this model, a nine-component food web model has been coupled with a wavelength-dependent subsurface irradiance model and a three-dimensional, primitive equation, regional circulation model. This model was developed for the CTZ with the overall objective of quantifying and understanding the physical and biological processes associated with the across-shore transport of nutrients and biomass.

The primary objective of this paper is to simulate the plankton dynamics observed while following a Lagrangian drifter as it becomes advected within the filament from nearshore to offshore. The resulting simulations are then used to determine which processes are responsible for creating the chemical and biological distributions observed while following a Lagrangian drifter as it is advected offshore within the CTZ.

The second section presents the methods used to calculate the velocities and resulting chemical and biological concentrations experienced by each of the two types of Lagrangian drifter experiments. The resulting values of the biological and chemical fields that the Lagrangian drifters experienced as they were advected offshore in a filament are presented in section 3. Finally, section 4 presents a discussion of the results and some conclusions.

2. Methods

2.1. One-Dimensional Lagrangian Drifter Experiment

The model used for the 1-D Lagrangian drifter experiments is a time- and depth-dependent physical and bio-optical model configured to simulate the plankton dynamics within the CTZ. A complete description of this model is presented by *Moisan and Hofmann* [this issue]. The model temperature and the nutrient and biological distributions were initialized with observations taken at the initial release point of a Lagrangian drifter which was released and followed in the CTZ study area in 1988 [*Abbott et al.,* 1990].

In using this 1-D model for Lagragian drifter simulations, we assumed that the effects of horizontal gradients were negligible. The approach further assumed that the nutrient and biological distributions along the drifter trajectory resulted from in situ processes and vertical advection only and that horizontal advective and diffusive processes were negligible.

The 1-D Lagrangian drifter model simulations were designed to investigate the vertical biological distributions that would be encountered along the trajectory of a Lagrangian drifter released in the CTZ at a point where it would be entrained in the offshore flowing filament. The simulated distributions obtained in this way can be compared to observations of nitrate, chlorophyll, and zooplankton concentrations made while following for 6 days a drifter that had been released as part of the 1988 CTZ field studies [*Hofmann et al.*, 1991].

Two separate simulations were carried out. In the first, the time- and depth-dependent vertical velocities were obtained from a simulated Lagrangian drifter. The chosen drifter used in the first simulation was one of 880 simulated Lagrangian drifters which were generated by a regional primitive equation circulation model that has been configured to simulate circulation conditions in the CTZ (Figure 1) [*Hofmann et al.*, 1991; *Haidvogel et al.*, 1991a]. The specific simulated Lagrangian drifter chosen was initially released in a region where an offshore-flowing filament was observed to form in the model. The path of the simulated Lagrangian drifter, after remapping to the drifter path, is shown in Figure 2a.

The vertical velocities experienced by the chosen simulated Lagrangian drifter were negative (downwelling) throughout the simulation (Figure 2b), and therefore the drifter was displaced vertically from its initial depth of 90 m to a final depth of approximately 170 m (Figure 2c). This deepening along the filament density front was observed to occur in the offshore flowing portion of the filament during the 1988 CTZ field surveys [*Washburn et al.*, 1991].

The upper 100-m depth-dependent vertical velocities from the 3-D circulation model [*Haidvogel et al.*, 1991a, b; *Moisan et al.*, this issue] are nearly linear, with maximal velocities at 100 m and zero velocity at the surface. A correlation coefficient of 0.93 was obtained from a linear fit of the simulated vertical velocities. In fact, the structure of the vertical velocity field in the upper ocean due to long wave-like processes is close to linear and decays to zero at the sea surface. Because of these simulation results and upper ocean observations, the vertical velocity field in the 1-D model simulations was set as follows.

The vertical velocity at the sea surface, the top of the model domain, was set to zero. The vertical velocity at

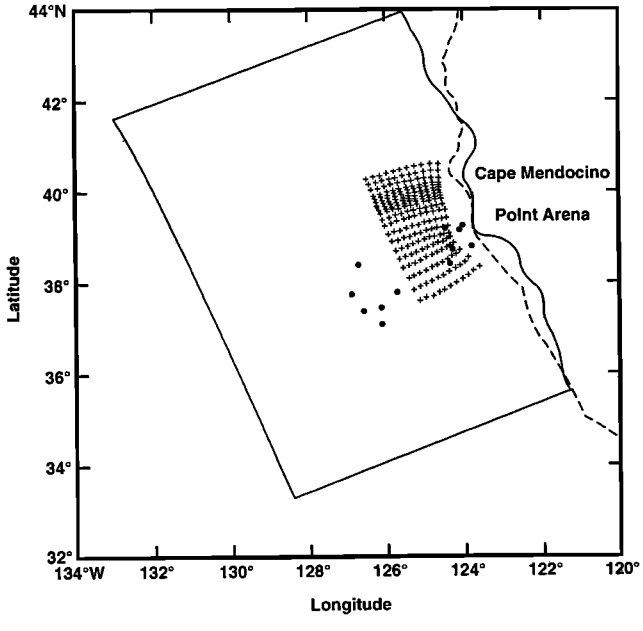

Figure 1. The CTZ study region. The region included in the CTZ circulation domain is indicated by the box. Within this domain, the release points for the Lagrangian drifter experiments are indicated by crosses. The dots indicate the stations at which nutrient, phytoplankton, and zooplankton measurements were made during the 1988 CTZ field sampling period. These stations follow along the track of a drifter that was deployed in an offshore flowing filament. The dashed line represents the actual coastal topography; the solid line represents the idealized coastal topography used in the circulation model.

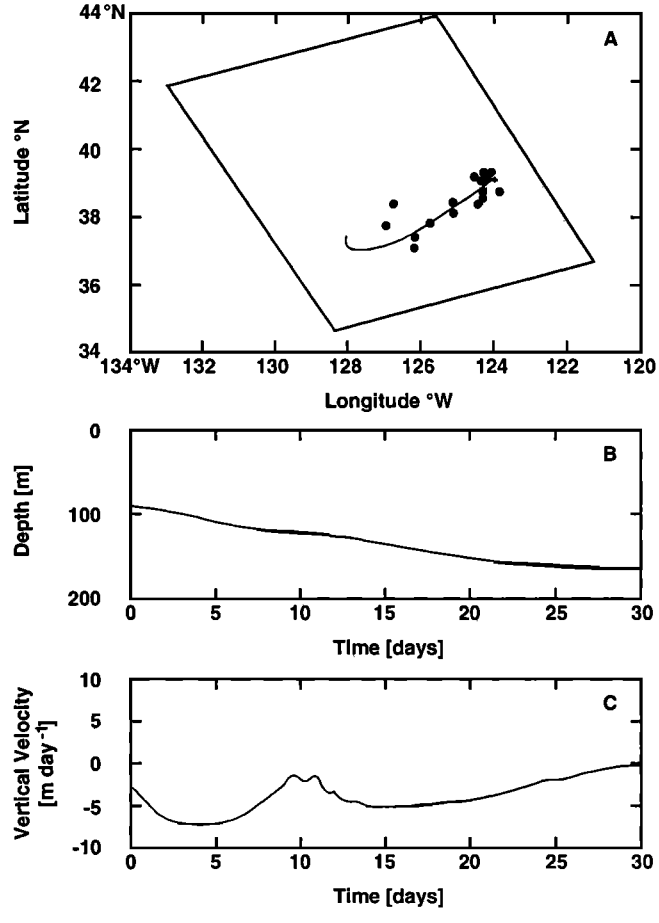

Figure 2. (a) The trajectory followed by the simulated Lagrangian drifter released near the region of the start of the actual drifter track. The dots indicate the stations at which nutrient, phytoplankton and zooplankton measurements were made during the 1988 CTZ field sampling period. (b) The vertical displacement of the simulated Lagrangian drifter over time. (c) The vertical velocity (m d^{-1}) experienced by the simulated Lagrangian drifter as it was advected offshore of the model domain.

100 m, the bottom of the domain, was prescribed as a time-varying vertical velocity and was obtained from the vertical velocity at 100 m observed by the simulated Lagrangian drifter as it was advected offshore while entrained within the filament. The vertical velocities were extracted from the simulated 3-D circulation fields at intervals of 4.8 hours and then linearly interpolated to the 5 minute time step used in this calculation.

The interior vertical velocities were obtained by assuming a linear dependence in the vertical between 0 and 100 m,

$$\frac{\partial w(z,t)}{\partial z} = \frac{w(z = 100\mathrm{m}, t) - w(z = 0\mathrm{m}, t)}{100\mathrm{m}}.$$

The interior vertical velocities were then obtained from:

$$w(z,t) = \frac{w(z = 100\mathrm{m}, t)}{100\mathrm{m}} z,$$

where z is the depth. This approach assumes a constant horizontal divergence throughout the upper 100 m, and also conserves mass.

As a comparison, a second simulation was performed in which no vertical advection was allowed. The simulations in both cases were extended for 20 days. However, measurements made during the 1988 field study cover a period of only 6 days. Therefore comparisons between the two can only be made for a short period of time. The resulting simulated chemical and biological distributions were compared to the data collected from stations sampled while following a Lagrangian drifter in the CTZ study area in 1988. The resulting simulated passive Lagrangian path allowed for tracing of the temporal evolution of the biological fields within a Lagrangian water parcel and provided an estimate of the time scales of the associated CTZ plankton populations.

2.2. Three-Dimensional Lagrangian Drifter Experiment

Simulated Lagrangian drifters, which served as passive tracers, were released into the 3-D, time-varying physical, biological, and chemical fields generated by the regional 3-D physical-bio-optical model presented by *Moisan et al.* [this issue]. The trajectories followed by these drifters and the magnitudes of the physical, chemical, and biological fields they encountered were then calculated.

The numerical technique used for determining the location of the Lagrangian floats at a given time is discussed in detail by *Hedström* [1990] and *Hofmann et al.* [1991]. Briefly, the distance traveled by a simulated drifter in a time interval was calculated using a fourth-order Runge-Kutta scheme:

$$\vec{k}_1 = \Delta t \times \vec{v}(t, \vec{x}_n) \quad (1)$$

$$\vec{k}_2 = \Delta t \times \vec{v}(t + \frac{\Delta t}{2}, \vec{x}_n + \frac{\vec{k}_1}{2}) \quad (2)$$

$$\vec{k}_3 = \Delta t \times \vec{v}(t + \frac{\Delta t}{2}, \vec{x}_n + \frac{\vec{k}_2}{2}) \quad (3)$$

$$\vec{k}_4 = \Delta t \times \vec{v}(t + \Delta t, \vec{x}_n + \vec{k}_3) \quad (4)$$

$$\vec{x}_{n+1} = \vec{x}_n + \frac{\vec{k}_1}{6} + \frac{\vec{k}_2}{3} + \frac{\vec{k}_3}{3} + \frac{\vec{k}_4}{6} \quad (5)$$

where $\vec{x}_{n+1}$ represents the new location of a particle that is advected from its previous position $\vec{x}_n$ by the velocity $\vec{v}$ in a time interval Δt, and $\vec{k}_i$ represents the Runge-Kutta coefficients.

These tracers were capable of moving within the grid boxes, and so the fluid velocities, $\vec{v}$, at points not represented by grid points were required for use in the Runga-Kutta scheme. The model obtained these velocities by using a horizontal, bicubic interpolation algorithm of the form

$$\vec{v}(x_f, y_f) = \sum_{i=1,4} \sum_{j=1,4} \vec{v}(x_i, y_j) \frac{\prod_{k=1,4}^{k \neq i} (x_f - x_k) \prod_{l=1,4}^{l \neq j} (y_f - y_l)}{\prod_{k=1,4}^{k \neq i} (x_i - x_k) \prod_{l=1,4}^{l \neq j} (y_j - y_l)}, \quad (6)$$

where (x_f, y_f) is the position of the Lagrangian drifter and (x_i, y_i) are the positions of the 16 neighboring grid points. The magnitudes of the chemical and biological fields encountered along the path of the drifter were also calculated using the above bicubic interpolation scheme.

Simulated Lagrangian drifter experiments were carried out between model day 140 and 160. A total of 880 drifters were released in the model domain at points which surrounded the location at which a filament was observed to form (Figure 1). Three sets of drifters were released at each location at depths of 30, 60, and 90 m and were followed for 20 days. The position of these drifters varied over time as a result of the vertical and horizontal velocities that they experienced. A fourth drifter set was released at each location; however, this drifter set was constrained to remain at 30 m. The position of this set of drifters varied over time only as a result of horizontal velocities.

The resulting paths taken by the simulated drifters also allow for vertical sampling of the 3-D fields as the drifters were advected through the model domain. This form of numerical data sampling was similar to the field sampling scheme used by *Abbott et al.* [1990] and *Mackas et al.* [1991], and thus the results from these are compared.

The final results obtained from the 3-D physical-bio-optical model consisted of extracting the biological and chemical distributions along trajectories followed by drifters released in the simulated circulation fields. Such an approach allows quantification of the changes in the biological and chemical fields while the water parcel moves from the nearshore neritic environment to offshore waters.

3. Results

3.1. One-Dimensional Lagrangian Drifter Experiment

The depth of the nutricline, defined as the depth of the 10 mg N m^{-3} isopleth, deepened for both conditions with and without vertical advection (Figure 3). How-

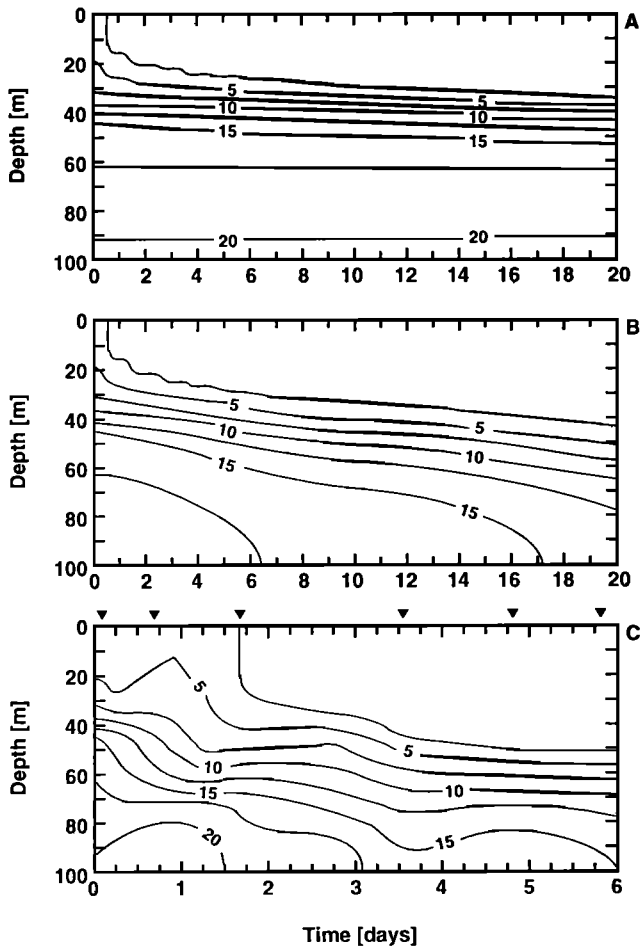

Figure 3. Time evolution of the simulated vertical nitrate distributions for conditions of (a) no vertical advection and (b) vertical advective field obtained from a circulation simulation for the CTZ, with (c) observed nitrate fields measured while following a drifter released during the 1988 CTZ field studies shown for comparison. Triangles at the top of Figure 3c indicate the times at which measurements were made. Values were obtained at intervening times by linear interpolation. Contour levels are 2.5 mg N m^{-3} for all panels. Note scale change in the time axis between Figures 3a and 3b, and 3c.

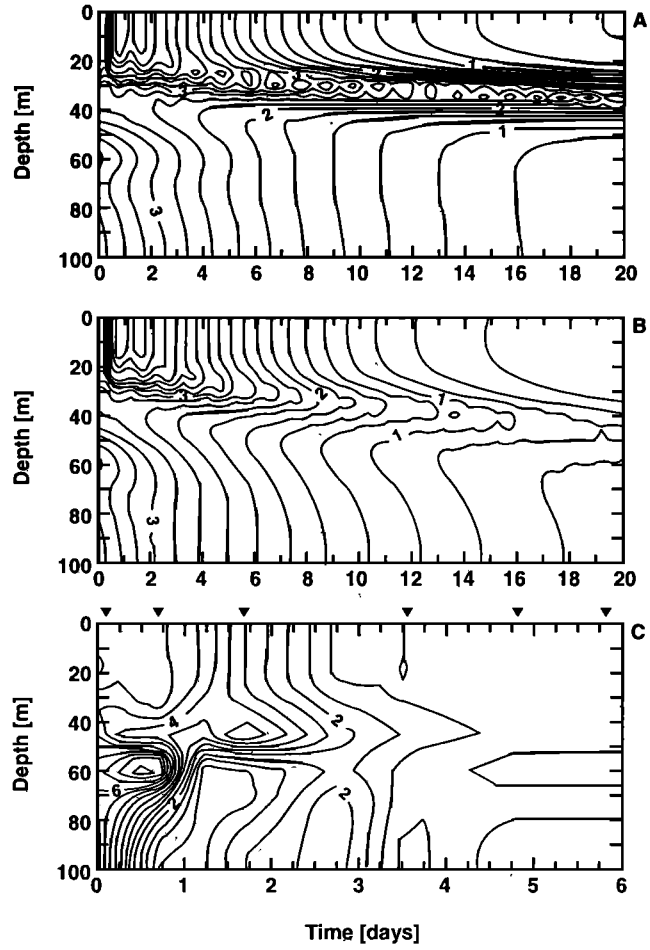

Figure 4. Time evolution of the simulated vertical chlorophyll distributions for conditions of (a) no vertical advection and (b) vertical advective field obtained from a circulation simulation for the CTZ, with (c) observed chlorophyll fields measured while following a drifter released during the 1988 CTZ field studies shown for comparison. Triangles at the top of Figure 4c indicate the times at which measurements were made. Values were obtained at intervening times by linear interpolation. Contour levels are 0.25 mg chl a m^{-3}, 0.25 mg chl a m^{-3} and 0.5 mg chl a m^{-3} for Figures 4a, 4b, and 4c, respectively. Note scale change in the time axis between Figures 4a and 4b, and Figure 4c.

ever, the final depth for the no-vertical-velocity simulation (45 m) was shallower than that for the vertical advection simulation (67 m). The observed depth of the nutricline (Figure 3c) deepened from 34 to 70 m during the 6 days covered by the field study. This rate of decrease is much faster than that simulated. Overall, the pattern in the observed nitrate field is closer to that obtained for the vertical advection case than for the no advection case.

The simulated chlorophyll fields obtained without (Figure 4a) and with (Figure 4b) vertical advection show the development of a subsurface chlorophyll maximum that deepens over the 20-day simulation. The rate of deepening is greater for the advective case, 1.5 m d^{-1} versus 0.75 m d^{-1}. A chlorophyll maximum was observed during the field study (Figure 4c) and deepened from about 15 to 45 m during the 6 days encompassed by the observations. The vertical distributions and rate of deepening of the observed chlorophyll distribution are similar to those obtained for the vertical advection case.

The rapid deepening of the nutricline and chlorophyll maximum in the distributions of the CTZ field studies has been attributed to downwelling vertical velocity rates of 20 to 30 m d^{-1} [*Kadko et al.*, 1991; *Washburn et al.*, 1991]. The maximum vertical velocities obtained in the simulated Lagrangian drifter from the CTZ circulation simulations (Figure 2) are about 7 m d^{-1}. Hence the simulated distributions will not deepen as rapidly as was observed. However, the overall patterns are similar, and the simulations with and without vertical advection

demonstrated the importance of this process in regulating the vertical distribution of biological quantities.

As a final comparison, the simulated reproductive effort for the three zooplankton species was obtained along the drifter track from the simulation that included vertical advection (Figure 5). The reproductive effort is defined as the amount of assimilated food remaining after growth, respiration, and molting that is available for use in reproduction. The simulated reproductive efforts for the copepod (*Eucalanus californicus*) and the euphausiid (*Euphausia pacificus*) are highest during the initial 6 to 7 days of the simulation, when the simulated drifter was in the nearshore region of the filament. In contrast, the doliolid (*Dolioletta gegenbauri*) showed the highest reproductive effort at the end of the simulation, when the drifter was located offshore. These simulated results are in qualitative agreement with the observations of zooplankton reproductive effort from the CTZ. Highest biomass and egg production rates for *E. californicus* and *E. pacificus* were found in the nearshore region of the filament [*Smith and Lane*, 1991; *Mackas et al.*, 1991]. The highest biomass of *D. gegenbauri* was found in the offshore regions [*Mackas et al.*, 1991]. Reproductive rates were not measured for this animal.

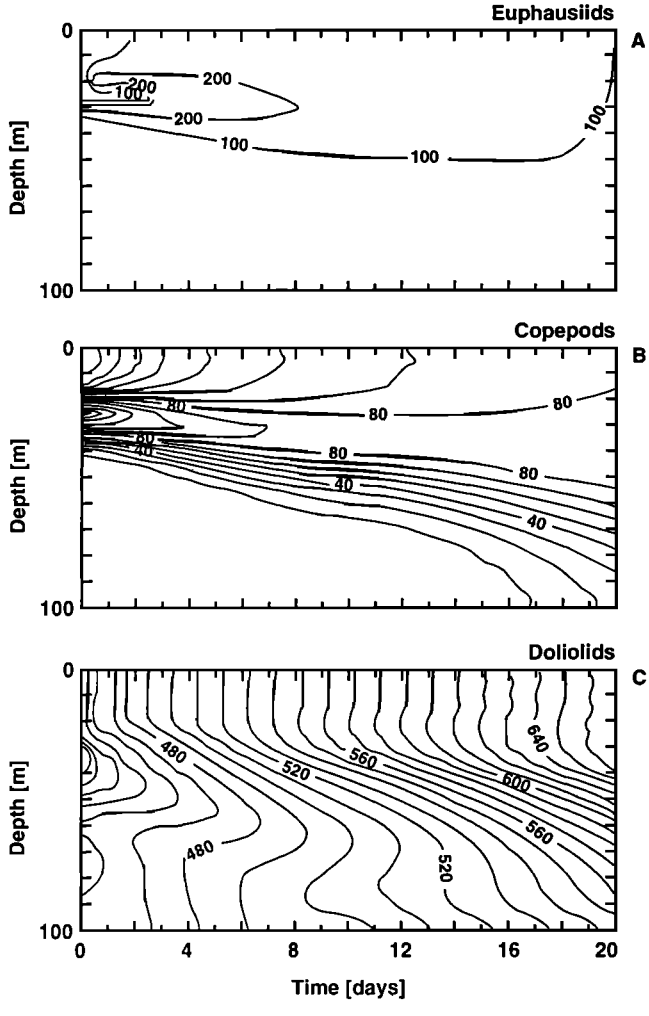

Figure 5. The 20-day time evolution of the simulated zooplankton reproductive effort (μg N m^{-3} d^{-1}) with depth for the vertical velocity case: (a) euphausiids, (b) copepods, and (c) doliolids. High reproductive rates were observed early in the simulation for the euphausiid and copepod fractions, when the drifter was within the region of filament formation. Conversely, the simulated reproductive rates for the doliolid fraction were highest at the end of the simulation, when the drifter was farthest from shore. Contour levels are 100 μg N m^{-3} d^{-1}, 10 μg N m^{-3} d^{-1}, and 10 μg N m^{-3} d^{-1}, for Figures 5a, 5b, and 5c, respectively.

3.2. Three-Dimensional Lagrangian Drifter Experiment

3.2.1. Composite drifter trajectories and velocities. The drifter array was initially positioned upstream of a filament that formed in the model region (Figure 1). This allowed drifters to be entrained in the filament as it developed and extended offshore. A detailed analysis of the general transport patterns and residence times derived from an analysis of these drifters is given by *Hofmann et al.* [1991]. However, a brief description is given here as a basis for the biological distributions given in the following section.

The general drifter patterns are shown in Plate 1. Most of the drifters released within 150 km of the coast were transported to the south with the southward flow of the California Current. Those drifters released farther offshore were transported offshore in the filament. Many of the drifters that were located along the southern side of the filament were returned to the coastal regions by the cyclonic flow that occurred there. Those drifters that reached the outer extent of the filament became entrained in either the cyclonic or anticyclonic eddies that formed at the offshore extent of this feature.

The vertical velocities experienced by the drifters released at 90 m (Plate 1b) show that those drifters that were entrained in the filament were downwelled as they were transported offshore. Maximum downwelling velocities ranged from 47 to 55 m d^{-1}. The minimum and maximum depths experienced by these drifters were 15.8 and 207.7 m, respectively. Upwelling velocities were experienced by drifters on the southern side of the filament and by those transported southward along the coast.

3.2.2. Biological distributions. The total phytoplankton concentrations along the drifter trajectories (Plate 2a) showed highest concentrations, about 392.5 mg C m^{-3}, at the onshore end of the trajectories. As the drifters moved offshore in the filament, phytoplankton concentrations decreased. A similar decrease in concentration with time occurred along the trajectories of drifters not entrained in the filament.

The phytoplankton populations at the onshore base of the filament initially consisted of primarily large cells (Plate 2b). As the drifters moved offshore in the filament, the relative abundance of the phytoplankton population shifted to dominance by the smaller size fraction. This change in dominance increased with increasing distance offshore. At the offshore extent of the filament, the phytoplankton populations to the south of the feature had a higher percentage of large phyto-

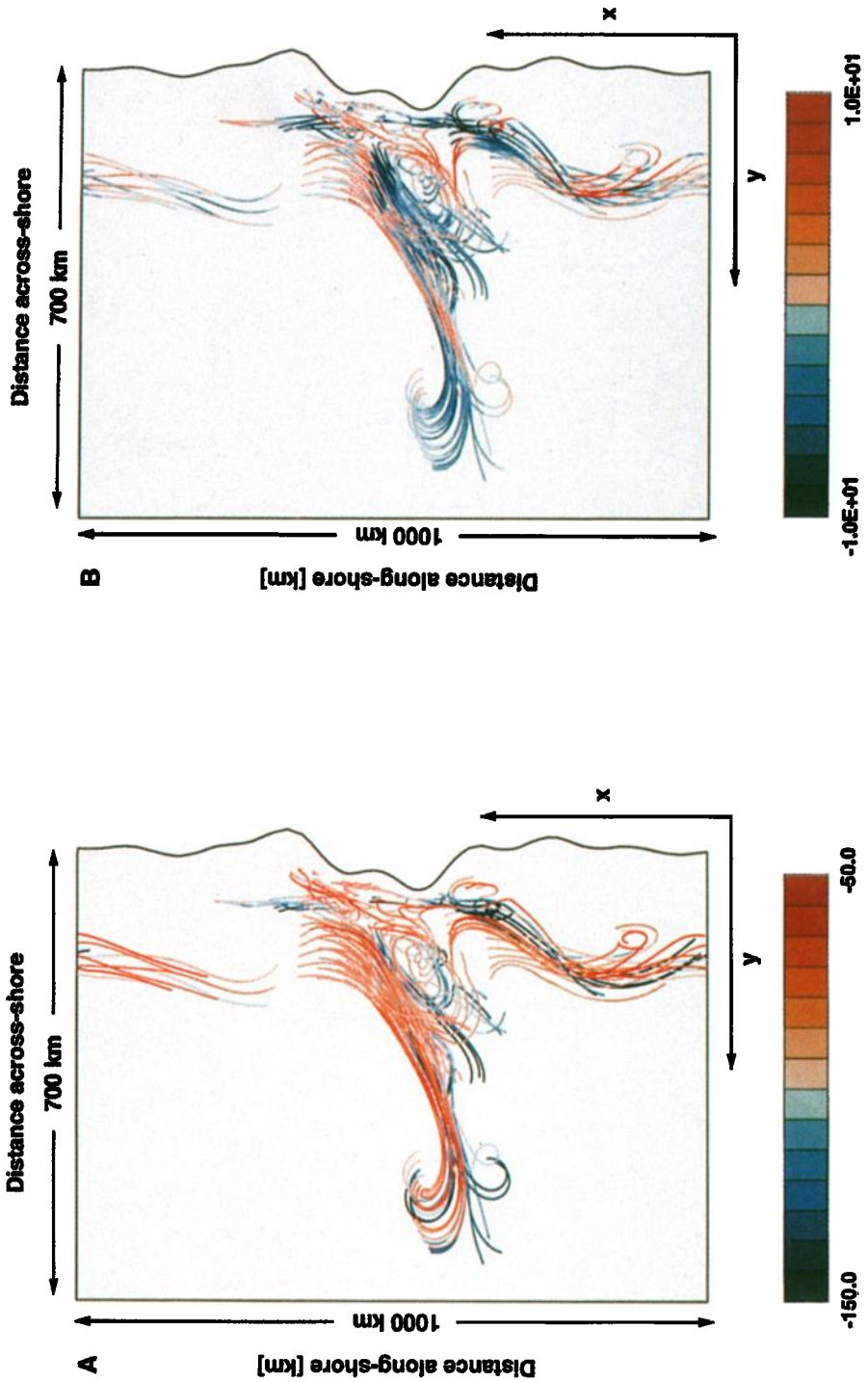

Plate 1. Composite of the simulated drifter trajectories. (a) Vertical displacement in meters along the trajectories of the variable depth drifters released at 90-m. Color along the trajectory indicates the depth in meters of the drifter and ranges from 207.7 m (dark blue) to 15.8 m (dark red). Any drifter depth deeper than 150.0 m is shown in dark blue, and any drifter depth shallower than 50.0 m is shown in dark red. (b) Vertical velocity in meters per day experienced by the variable depth 90-m drifters along their trajectories. Color along the trajectory indicates the magnitude of the vertical velocity ($m\ s^{-1}$), and the colors are chosen to show details of the vertical velocity, which ranges from -47 $m\ d^{-1}$ (dark blue) to 55 $m\ d^{-1}$ (dark red). Any vertical velocity larger than 10 $m\ d^{-1}$ is shown in dark blue, and any smaller than -10 $m\ d^{-1}$ is shown in dark red.

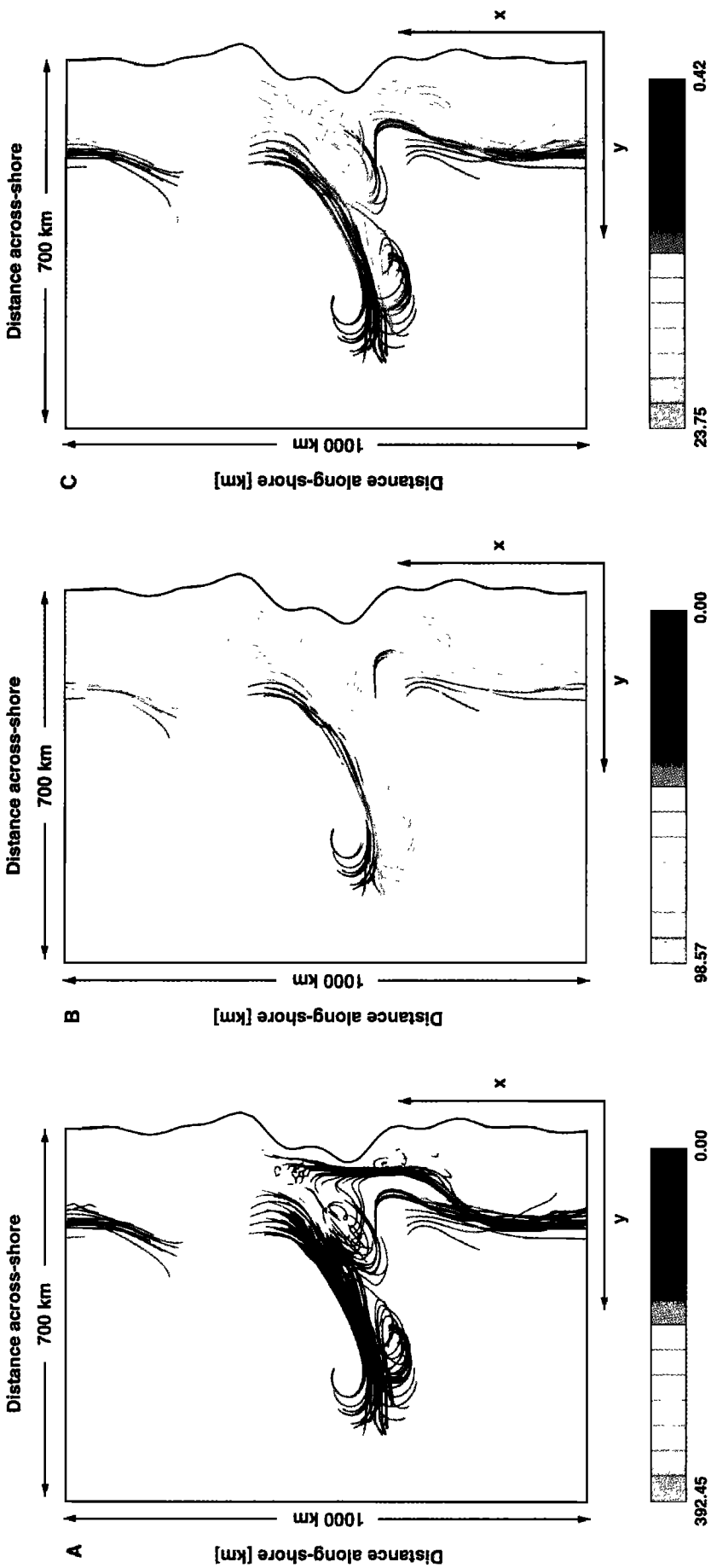

Plate 2. Composite of the simulated drifter trajectories released at 90 m. Color along the trajectories indicates (a) the concentration of large and small phytoplankton (0 mg C m^{-3} (dark blue) to 392.45 mg C m^{-3} (dark red)), (b) the percent of large phytoplankton to total phytoplankton (0 (dark blue) to 98.57 (dark red)), and the total zooplankton biomass (0.42 mg C m^{-3} (dark blue) to 23.75 mg C m^{-3} (dark red)).

plankton cells than those to the north. This reflects the differing nutrient environments that are produced by cyclonic and anticyclonic circulations. The anticyclonic circulation on the northern side of the filament is formed from nutrient-poor, low phytoplankton biomass water, while the cyclonic circulation on the southern side of the filament is formed from the nutrient-rich, high phytoplankton biomass water from the core of the filament.

In general, zooplankton concentrations encountered along the drifter trajectories (Plate 2c) were similar to those obtained for the phytoplankton concentrations. Highest concentrations were inshore and decreased concentrations were found along the filament and in offshore waters. The zooplankton populations inshore of the filament were composed of about 40% ($\approx$ 9.5 mg C m^{-3}) euphausiids, 40% ($\approx$ 9.5 mg C m^{-3}) copepods, and 20% ($\approx$ 4.8 mg C m^{-3}) doliolids. Within the filament, copepods were more dominant, with about 43% ($\approx$ 6.5 mg C m^{-3}) copepods, 19% ($\approx$ 2.9 mg C m^{-3}) euphausiids, and 37% ($\approx$ 5.5 mg C m^{-3}) doliolids. Within the offshore portion of the filament, the copepods continued to remain dominant, with about 55% ($\approx$ 0.23 mg C m^{-3}) copepods, 33% ($\approx$ 0.14 mg C m^{-3}) euphausiids, and 11% ($\approx$ 0.05 mg C m^{-3}) doliolids.

The vertical structure of the phytoplankton and zooplankton distributions in the upper 1000 m of the water column along the trajectory of a drifter that was transported offshore in the filament is shown in Figures

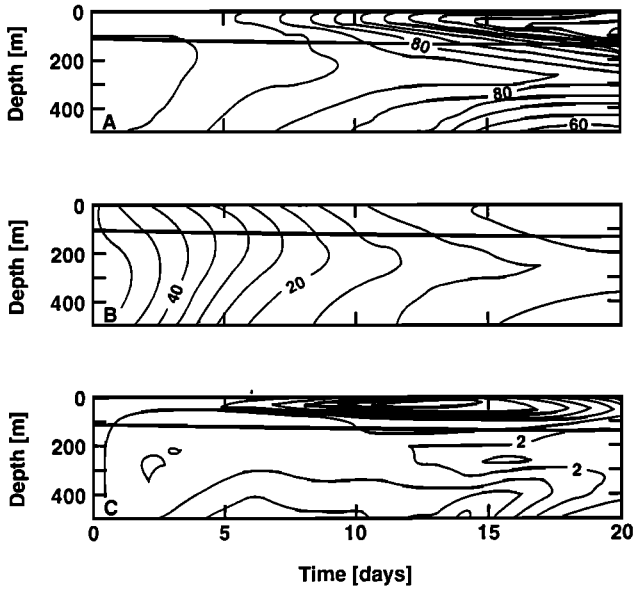

Figure 6. The depth-dependent fields of the (a) percent of large to total phytoplankton concentration, and the concentrations (mg N m^{-3}) of (b) large and (c) small phytoplankton size fractions sampled above and below a Lagrangian drifter as it was advected offshore within the filament. The solid line located initially at 90 m indicates the depth to which the drifter moved over time. This particular drifter was released at 90 m and allowed to vary in depth in response to the vertical velocities it experienced. Contour levels are 5%, 5 mg N m^{-3}, and 0.5 mg N m^{-3} for Figures 6a, 6b, and 6c, respectively.

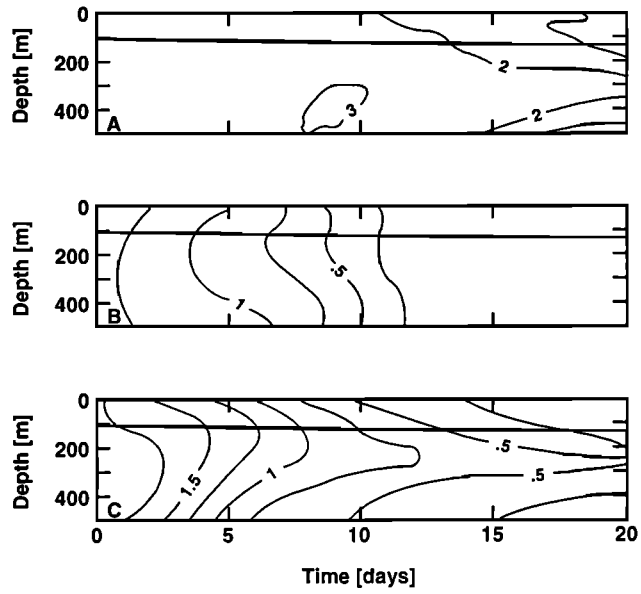

Figure 7. The depth-dependent fields of the (a) copepod, (b) doliolid, and (c) euphausiid concentrations (mg N m^{-3}) sampled above and below a Lagrangian drifter as it was advected offshore within the filament. The solid line initially located at 90 m indicates the depth to which the drifter moved over time. This particular drifter was released at 90 m and allowed to vary in depth in response to the vertical velocities it experienced. Contour levels are 1 mg N m^{-3}, 0.25 mg N m^{-3}, and 0.25 mg N m^{-3}, for Figures 7a, 7b, and 7c, respectively.

6 and 7. Initially, the phytoplankton population was dominated by the fast growing, silicate-dependent, large phytoplankton assemblage (Figure 6a). However, grazing and nutrient depletion reduced the concentration of this size fraction over time and with increased distance offshore. At the offshore end of the trajectory at model day 160, the small phytoplankton fraction dominated at depth. The large cells still accounted for the majority of the phytoplankton biomass above 100 m, but overall, the large phytoplankton were less dominant than that observed in the coastal regions. The subsurface chlorophyll maximum associated with the large phytoplankton size fraction deepened along the drifter trajectory. This may have contributed to the apparent decrease in chlorophyll biomass at the offshore extent of the drifter trajectory.

The zooplankton distributions along the drifter trajectory showed increased copepod (Figure 7a) and euphausiid (Figure 7b) concentrations at the offshore end of the filament between 200 and 400 m. Doliolid (Figure 7b) populations were confined primarily to the more onshore portions of the trajectory.

4. Discussion and Conclusions

4.1. One-Dimensional Lagrangian Drifter Experiment

Moisan and Hofmann [this issue] used a vertical- and time-dependent bio-optical model to simulate the bio-

logical and physical processes which control the time development of the vertical distributions of the nutrient and plankton fields within the CTZ. The results from this study demonstrated that the development and maintenance of the subsurface chlorophyll maximum was primarily controlled by phytoplankton in situ growth and that its depth covaried with the depth of the nutricline. In general, the chlorophyll maximum was approximately 10 m nearshore and deepened to more than 65 m farther offshore. Coastal water entrained within the offshore flowing portion of a filament will develop a deeper subsurface chlorophyll layer as it becomes incorporated into the offshore water mass.

Downwelling along the northern offshore-flowing side of the filament was observed to be as high as 20 to 40 m d^{-1} [*Kadko et al.*, 1991; *Dewey et al.*, 1991]. This rapid subduction of water has a considerable effect on the plankton dynamics. Results from the model simulations show that downwelling vertical velocities cause the nutricline and chlorophyll maximum to develop at greater depths (Figures 3 and 4). *Washburn et al.* [1991] suggested that the phytoplankton in the water column within the filament may have been downwelled over 100 m as they were advected offshore while entrained within the filament. Also, *Abbott et al.* [1990] favored the explanation that downwelling was partly responsible for the optical and biological properties measured by a fixed-depth drifter as it was advected offshore while entrained within a filament. The presence of a deficiency in the concentration of ^{226}Rn within the water column along the front of the filament, along with the presence of a chlorophyll layer well below the euphotic zone led *Kadko et al.* [1991] to estimate that the rate of downwelling along the offshore-flowing portion of the filament was approximately 25 m d^{-1}. The downwelling of water in the model also caused the euphotic zone to deepen and the f ratio to decrease as the supply of new nutrients decreased. For upwelling simulations, the effect was reversed.

High reproductive efforts in the copepod *E. californicus* have previously been observed off the California coast [*Smith et al.*, 1986] and within the filament [*Smith and Lane*, 1991]. Copepod and euphausiid populations in the model simulations had higher reproductive effort in regions with high concentrations of the fast-growing, large phytoplankton. These regions coincided with regions where silicate concentrations were less limiting to these fast-growing, silicate-dependent phytoplankton.

4.2. Three-Dimensional Lagrangian Drifter Experiment

By using simulated Lagrangian drifters in conjunction with a coupled physical-bio-optical model, the effects of in situ processes can be separated from the advective effects of the circulation field. The numerical experiments show that the time development of the biological and chemical constituents while following a Lagrangian drifter can be quite variable. This is partly due to the initial conditions that the simulated Lagrangian drifters were given. The drifters released closer to shore were initialized with higher nutrient concentrations, greater phytoplankton biomass dominated by the large, fast growing diatoms, and a large zooplankton population composed primarily of euphausiids, some copepods, and few doliolids. The drifters released over the shelf break were initialized with lower nutrient concentrations, a lower phytoplankton biomass containing equal amounts of both phytoplankton fractions, and a smaller zooplankton population dominated by the doliolid population. Those drifters released farthest offshore were initialized with low nutrient concentrations, a low phytoplankton biomass composed primarily of the slow growing, small population, and a small zooplankton population composed primarily of doliolids and copepods.

The initial positions of the simulated Lagrangian drifters were also important in determining what the Lagrangian drifters experienced. *Hofmann et al.* [1991] showed that the ultimate fate of the simulated Lagrangian drifters depended upon how close the drifters were released to the formation region of the filament. Of the 880 simulated Lagrangian drifters released during the simulation, a total of 279 were entrained within the rapid offshore flowing portion of the filament and were advected offshore more than 400 km (Plate 1). In general, these drifters all experienced similar changes in the concentrations of the biological and chemical constituents in the water column. The fast-growing (neritic) phytoplankton population dominated the water column at the onshore portion of the simulated Lagrangian drifter tracks. As the simulated Lagrangian drifters were advected offshore, both populations decreased in magnitude (Plate 2a) due to the loss of nutrients, grazing, and death. The slow growing (oceanic) small phytoplankton population became more dominant (Plate 2b). This progressive change in the phytoplankton populations from fast growing and neritic to slow growing and oceanic was also partly observed in the CTZ while following an Lagrangian drifter as it was advected offshore within a filament [*Abbott et al.*, 1990].

If we compare the composite trajectories of the simulated Lagrangian drifters (Plate 2) to the quasi-synoptic observations from the CTZ program, similar patterns emerge. Of the simulated Lagrangian drifters which were advected offshore, a rapid change in the cross-filament direction occurred in the nutrient, phytoplankton and zooplankton, fields. High nutrient and phytoplankton concentrations occurred within the slow moving core of the filament. Moving from the slow flowing core to the offshore flowing portion of the filament, a sharp transition occurs from high to low nutrient and phytoplankton concentrations. Highest concentrations of zooplankton were found in the core due to the advection of water containing high zooplankton concentrations from the shelf region. Offshore, the biomass and nutrient concentrations all decreased. *Hood et al.* [1990] and *Chavez et al.* [1991] both observed similar patterns in the nutrient and phytoplankton fields. Both nutrient and phytoplankton populations decreased from the slow flowing core of the filament to the offshore, with the sharpest gradient within the fast flowing portion of the filament.

Mackas et al. [1991] presented results from a study which looked at zooplankton distributions within an offshore flowing filament. Zooplankton samples were obtained by sampling the water column while following a Lagrangian drifter which was released into the offshore flowing region of the filament. The observed zooplankton distributions were banded parallel to the axis of the filament, with highest concentrations, primarily composed of *Euphausia pacifica*, occurring within the cold regions of the filament where offshore velocities were slowest. *Eucalanus californicus*, and euphausiid larvae dominated the water in the region where the filement showed highest offshore velocities. *Mackas et al.* [1991] also observed a rapid change in the zooplankton assemblage across the filaments, with highest concentrations within the filament. As in our results, *Mackas et al.* [1991] found that a core group of samples matched the trajectories of several drifters which were released upstream of the filament. In the offshore regions, the zooplankton assemblage was composed primarily of chaetognaths, heteropod larvae, *Dolioletta gegenbauri*, and a mixture of small copepods.

Furthermore, *Smith and Lane* [1991] found highest rates of egg production for the copepod *E. californicus* in the filament to occur within the cold slow-flowing portion, where the high concentrations of phytoplankton biomass are observed. High rates of egg production was observed (not shown) onshore and within the slow flowing core of the filament for both the euphausiid and copepod populations. Since egg production is directly linked to food availability, this result is expected. This high secondary production within the slow-moving core of the filament may help to explain the high zooplankton biomass observed to exist approximately 200 km offshore in the southern region of the CTZ [*Chelton et al.*, 1982].

This study used simulated Lagrangian drifters to estimate the in situ biological and chemical character of water parcels as they were entrained and advected offshore within a filament. Such numerically derived calculations can be accomplished only with a realistic circulation field and initial conditions. Simulated drifters can be deployed into coupled physical-bio-optical models to give estimates of the in situ processes which control the time development of the ecosystem within the water parcels as they are advected along with the circulation field.

With the increasing use of instrumented Lagrangian drifters equipped with physical, biological, and optical sensing instruments to acquire data on the world ocean and the development of data assimilation techniques, simulated Lagrangian drifters should continue to be used with coupled physical-biological models as another tool to investigate the interactions between the circulation field and the ecosystem which interacts with it.

Acknowledgments. We thank D. B. Haidvogel for allowing us to use his semi-spectral primitive equation model (SPEM) and results obtained from it for the CTZ and for providing us with much needed advice. Special thanks go to K. S. Hedström for helping us to understand and use the SPEM code and its simulated drifter routines. We thank R. Bidigare, R. Hood, S. Smith, D. Mackas, L. Washburn, B. Jones, C. Davis, F. Chavez, J. Huyer, C. Paulson, and others within the CTZ group for providing us with the wealth of data used to complete this study. This research was supported by the Office of Naval Research under grant N00014-90-J-1930. Computer resources and facilities were provided by the Commonwealth Center for Coastal Physical Oceanography, Naval Research Laboratory, and Stennis Space Center. This support is gratefully acknowledged. This research was performed by J.R.M. in partial fulfillment of the requirements for a Ph.D. degree at Old Dominion University.

References

Abbott, M. R., K. H. Brink, C. R. Booth, D. Blasco, L. A. Codispoti, P. P. Niiler, and S. R. Ramp, Observations of phytoplankton and nutrients from a Lagrangian drifter off northern California, *J. Geophys. Res.*, *95*, 9393-9409, 1990.

Brink, K. H., and T. J. Cowles, The Coastal Transition Zone program, *J. Geophys. Res.*, *96*, 14,637-14,647, 1991.

Brink, K. H., R. C. Beardsley, P. P. Niiler, M. Abbott, A. Huyer, S. Ramp, T. Stanton, and D. Stuart, Statistical properties of near-surface flow in the California coastal transition zone, *J. Geophys. Res.*, *96*, 14,693-14,706, 1991.

Chavez, F., R. T. Barber, A. Huyer, P. M. Kosro, S. Ramp, T. Stanton, and B. Rojas de Mendiola, Horizontal transport of nutrients in the coastal transition zone off northern California: Effects on primary production, phytoplankton biomass, and species composition, *J. Geophys. Res.*, *96*, 14,809-14,831, 1991.

Chelton, D. B., P. A. Bernal, and J. A. McGowan, Large-scale interannual physical and biological interaction in the California Current *J. Mar. Res.*, *40*, 1095-1125, 1982.

Data Buoy Cooperation Panel, Surface Velocity Program drifting buoy cooperation panel workshop on evaluation of low cost barometer drifters, edited by L. Sombardier, *Scripps Inst. of Oceanogr. Series 93/28, WOCE Rep. No.* 108/93, Scripps Inst. of Oceanogr., La Jolla, Calif., 1993.

Davis, R. E., Drifter observations of coastal surface currents during CODE: The method and descriptive view, *J. Geophys. Res.*, *90*, 4741-4755, 1985a.

Davis, R. E., Drifter observations of coastal surface currents during CODE: The statistical and dynamical views, *J. Geophys. Res.*, *90*, 4756-4772, 1985b.

Dewey, R. K., J. N. Moum, C. A. Paulson, D. R. Caldwell, and S. D. Pierce, Structure and dynamics of a coastal filament, *J. Geophys. Res.*, *96*, 14,885-14,907, 1991.

Flament, P., Subduction and finestructure associated with upwelling filaments, Ph.D. thesis, 123 pp., Scripps Inst. of Oceanogr., La Jolla, Calif., 1986.

Haidvogel, D. B., A. Beckmann, and K. S. Hedström, Dynamical simulations of filament formation and evolution in the coastal transition zone, *J. Geophys. Res.*, *96*, 15,017-15,040, 1991a.

Haidvogel, D. B., J. Wilkin, and R. E. Young, A semi-spectral primitive equation ocean circulation model using vertical sigma and orthogonal curvilinear coordinates, *J. Comput. Phys.*, *94*, 151-185, 1991b.

Hedström, K. S., User's manual for a semi-spectral primitive equation regional ocean-circulation model, version 3. 0, Tech. Note FY90-2, 82 pp., Inst. of Nav. Ocean., Stennis Space Cent., Miss., 1990.

Hofmann, E. E., K.S. Hedström, J.R. Moisan, D.B. Haidvogel, and D. L. Mackas, The use of simulated drifter tracks

to investigate general transport patterns and residence times in the coastal transition zone, *J. Geophys. Res.*, *96*, 15,041-15,052, 1991.

Hood, R., M. Abbott, A. Huyer, and P. Kosro, Surface patterns in temperature, flow, phytoplankton biomass, and species composition in the coastal transition zone off northern California *J. Geophys. Res.*, *95*, 18,081-18,094, 1990.

Kadko, D. C., L. Washburn, and B. Jones, Evidence of subduction within cold filaments of the northern California coastal transition zone, *J. Geophys. Res.*, *96*, 14,909-14,926, 1991.

Mackas, D. L., L. Washburn, and S. Smith, Zooplankton community pattern associated with a California Current cold filament, *J. Geophys. Res.*, *96*, 14,781-14,797, 1991.

Moisan, J. R., and E. E. Hofmann, Modeling nutrient and plankton processes in the California coastal transition zone, 1, A time- and depth-dependent model, *J. Geophys. Res.*, this issue.

Moisan, J. R., E. E. Hofmann, and D. B. Haidvogel, Modeling nutrient and plankton processes in the California coastal transition zone, 2, A three-dimensional physical-bio-optical model, *J. Geophys. Res.*, this issue.

Niiler, P. P., P. M. Poulain, and L. R. Haury, Synoptic three-dimensional circulation in an onshore-flowing filament of the California Current, *Deep Sea Res.*, *36*, 385-405, 1989.

Paduan, J. D., and P. P. Niiler, A Lagrangian description of motion in northern California coastal transition filaments, *J. Geophys. Res.*, *95*, 18,095-18,109, 1990.

Paduan, J. D., and P. P. Niiler, Structure of velocity and temperature in the northeast Pacific as measured with Lagrangian drifter in fall 1987, *J. Phys. Oceanogr.*, *23*, 585-600, 1993.

Smith, S. L., and P. V. Z. Lane, The jet off Point Arena, California: Its role in secondary production of the copepod *Eucalanus californicus* Johnson, *J. Geophys. Res.*, *96*, 14,849-14,858, 1991.

Smith, S. L., B. H. Jones, L. P. Atkinson, and K. H. Brink, Zooplankton in the upwelling fronts off Point Conception, California, in *Marine Interfaces Ecohydrodynamics, Elsevier Oceanogr. Ser.*, vol. 42, edited by J. C. J. Nihoul, pp. 195-213, Elsevier, New York, 1986.

Swenson, M. S., P. P. Niiler, K. H. Brink, and M. R. Abbott, Drifter observations of a cold filament off Point Arena, California, in July 1988, *J. Geophys. Res.*, *97*, 3593-3610, 1992.

Washburn, L., D. C. Kadko, B. H. Jones, T. Hayward, P. M. Kosro, T. P. Stanton, S. Ramp, and T. Cowles, Water mass subduction and the transport of phytoplankton in a coastal upwelling system, *J. Geophys. Res.*, *96*, 14,927-14,945, 1991.

E. E. Hofmann, Center for Coastal Physical Oceanography, Department of Oceanography, Old Dominion University, Norfolk, VA 23529.

J. R. Moisan, Physical Oceanography Research Division, Scripps Institution of Oceanography, La Jolla, CA 92093-0230. (e-mail moisan@vanilla.ucsd.edu)

(Received September 22, 1995; revised May 9, 1996; accepted May 23, 1996.)